

Spin-State Energetics and Spin-Crossover Behavior of Pseudotetrahedral Cobalt(III)–Imido Complexes. The Role of the Tripodal Supporting Ligand

Ingar H. Wasbotten and Abhik Ghosh*

Center for Theoretical and Computational Chemistry, Department of Chemistry, University of Tromsø, N-9037 Tromsø, Norway

Received March 21, 2007

DFT calculations have underscored the importance of the tripodal supporting ligand in tuning the spin-state energetics of pseudotetrahedral transition metal imido complexes. In particular, we have focused on Co(III)–imido complexes, where our best estimate (OLYP) of the singlet–triplet splitting varies from 0.75 eV for a trisphosphine complex (**1**) and 0.3 eV for a tris(*N*-heterocyclic-carbene) complex (**2**) to essentially 0.0 eV for a hydrotris(pyrazolyl)borate (**3**) complex. The experimentally studied analogues of **1**, **2**, and **3** all exhibit $S = 0$ ground states; however, the experimental analogue of **3** exhibits spin-crossover behavior due to a low-lying $S = 1$ state. Interestingly, whereas all the pure functionals examined successfully predict nearly equienergetic singlet and triplet states for **3**, the hybrid functionals B3LYP and O3LYP exhibit a clear (and incorrect) preference for the $S = 2$ state. In addition, we have also carried out an exploratory survey of Cr(III), Mn(III), and Fe(III) imido complexes with trisphosphine and hydrotris(pyrazolyl)borate (Tp) supporting ligands. Among the more interesting predictions of this study is that an Fe^{III}(Tp)(imido) species should exhibit a high-spin $S = 5/2$ ground state, which would be unique for an iron–imido complex.

Introduction

Middle and late transition metal imido complexes were largely unknown until very recently, which should not be surprising in light of the prohibitive d_{π} – p_{π} antibonding interactions that many such species would necessarily involve. Recently, however, the use of low-coordinate architectures has allowed the isolation and even structural characterization of a number of Fe, Co, and Ni imido complexes.¹ The great potential of these complexes for C–H activation and nitrene transfer chemistry, their relevance as models of nonheme metalloenzyme intermediates, and the novelty of their electronic structures are all leading to the recognition of this area as a major new advance in inorganic chemistry. The pseudotetrahedral or trigonal-planar coordination geometries of these complexes provide energetically accessible d_{δ} orbitals and a curiously low-energy d_{σ} orbital,^{2,3} thereby avoiding, as far as possible, occupancy of the high-

energy d_{π} – p_{π} antibonding orbitals (the σ , π , and δ descriptions being relative to the metal–imido linkage). Not surprisingly, therefore, low-coordinate Co^{III}–imido complexes generally exhibit low-spin $d^6 S = 0$ ground states.

Against this backdrop, the recent report⁴ of the apparently paramagnetic complex Co^{III}(Tp^{*t*Bu,Me})(NAd) (Tp^{*t*Bu,Me} = hydrotris(3-*t*-butyl-5-methylpyrazol-1-yl)borate, Ad = 1-Adamantyl) appeared surprising, prompting us to undertake a quantum chemical study of the system. The apparent paramagnetism of this species was in sharp contrast to the clear diamagnetism of the three other Co^{III}–imido complexes in the literature, which have trisphosphine,⁵ tris(*N*-heterocyclic-carbene),⁶ and β -diketiminato⁷ (nacnac) supporting ligands. Subsequently, it became clear that the assignment of an open-shell ground state for Co^{III}(Tp^{*t*Bu,Me})(NAd) was a

* To whom correspondence should be addressed. E-mail: abhik@chem.uit.no.

(1) Mehn, M. P.; Peters, J. C. *J. Inorg. Biochem.* **2006**, *100*, 634–643.
(2) Tangen, E.; Conradie, J.; Ghosh, A. *J. Chem. Theory Comput.* **2007**, *3*, 448–457.
(3) Conradie, J.; Ghosh, A. *J. Chem. Theory Comput.* **2007**, *3*, 689–702.

(4) (a) Shay, D. T.; Yap, G. P. A.; Zakharov, L. N.; Rheingold, A. L.; Theopold, K. H. *Angew. Chem., Int. Ed.* **2005**, *44*, 1508–1510. (b) Corrigendum: Shay, D. T.; Yap, G. P. A.; Zakharov, L. N.; Rheingold, A. L.; Theopold, K. H. *Angew. Chem., Int. Ed.* **2006**, *45*, 7870–7870.
(5) Jenkins, D. M.; Di Bilio, A. J.; Allen, M. J.; Betley, T.; Peters, J. C. *J. Am. Chem. Soc.* **2002**, *124*, 15336–15350.
(6) Hu, X.; Meyer, K. *J. Am. Chem. Soc.* **2004**, *126*, 16322–16323.
(7) Dai, X.; Kapoor, P.; Warren, T. H. *J. Am. Chem. Soc.* **2004**, *126*, 4798–4799.

mistake.^{4b} Despite the confusion, this complex is nonetheless of unusual interest: alone among known Co^{III}–imido complexes, Co^{III}(Tp^{tBu,Me})(NAd) exhibits spin-crossover behavior, i.e., a low-lying paramagnetic excited state.

These developments led us to undertake a computational examination of this entire area. To start with, we wanted to characterize the HOMO–LUMO gaps and the spin-state energetics of the various known pseudotetrahedral Co^{III}–imido complexes as a function of different supporting ligands. Although density functional theory (DFT) appears to be the obvious choice for such a study, the method is not without pitfalls. Thus, many common functionals provide an unreliable description of the energetics of the low-lying spin states of transition metal complexes.^{8,9} On a positive note, however, we were intrigued by the possibility that these complexes would furnish a challenging test of the performance of various functionals vis-à-vis transition metal spin-state energetics. These hopes were indeed fulfilled, and our study has yielded substantial insights into the spin-state energetics of these compounds, as well as an evaluation of the relative merits of various commonly used functionals.

Having obtained a “feel” for the performance of different functionals, we carried out an exploratory survey of Cr(III), Mn(III), and Fe(III) imido complexes with trisphosphine and hydrotris(pyrazolyl)borate (Tp) supporting ligands. Once again, the results underscore the critical role of the tripodal supporting ligands. In particular, we encountered multiple instances where our best computational estimates predict different ground spin states, depending on whether the supporting ligand is trisphosphine or Tp.

Methods

The various complexes studied were optimized with the OLYP^{10,11} generalized gradient approximation (GGA) and in some cases also the PW91¹² GGA, triple- ζ plus polarization Slater-type orbital basis sets and a fine mesh for numerical integration of matrix elements, as implemented in the ADF 2005¹³ program system. In addition, we also carried out single-point noniterative post-self-consistent-field (SCF) calculations with a variety of pure and hybrid functionals, namely, BLYP,^{14,15} RPBE,¹⁶ revPBE,¹⁷ mPBE,¹⁸ OPBE,^{10,19,20} B3LYP(VWN5),^{21–23} and O3LYP(VWN5).^{22,24} Unless otherwise indicated, the VWN functional was used as the local part of all of the above functionals.

As far as pseudotetrahedral Co(III)–imido complexes are concerned, we carried out both PW91 and OLYP optimizations of

the lowest-energy $S = 0, 1,$ and 2 states of the following three complexes using both the OLYP and PW91 GGAs: Co^{III}(mebp3)-(NMe) (**1**, mebp3 = methyltris(dimethylphosphinomethyl)borate),⁵ [Co^{III}(timen)(NPh)]⁺ (**2**, timen = tris[2-(3-phenylimidazol-2-ylidene)ethyl]amine),⁶ and Co^{III}(Tp^{tBu,Me})(N^tBu) (**3**).⁴ Each of these complexes is slightly simplified relative to the actual system studied experimentally but not in a way that should significantly affect the spin-state energetics. In addition to carrying out fully unconstrained optimizations for all the species studied, we also optimized **1** and **3** with C_{3v} constrained optimizations.

For the other metal–imido complexes, we considered only the mebp3 and Tp^{tBu,Me} supporting ligands and the following N^tBu complexes: Cr(III), $S = 3/2$; Mn(III), $S = 0, 1, 2$; Fe(III), $S = 1/2, 3/2, 5/2$. An OLYP optimization was carried out for each spin state, followed by post-SCF calculations at the optimized geometry with a variety of functionals, as mentioned above.

Results and Discussion

a. Co(III)–Imido Bonding. Figures 1, 2, and 3 depict highlights of the optimized geometries and other calculated results for **1**, **2**, and **3**, respectively. The optimized structures are generally in good agreement with experiment and do not merit extensive discussion. Briefly, the optimized (OLYP) ground-state Co–N_{imido} distances of 1.648, 1.672, and 1.656 Å in **1**, **2**, and **3** are in excellent agreement with corresponding experimentally observed distances of 1.658(2),⁵ 1.675–(2),⁶ and 1.655 Å,⁴ respectively. For **1** and **3**, the C_{3v} and symmetry-unconstrained optimized structures proved indistinguishable. However, **2** exhibits a mild bending of the imido linkage (OLYP \angle Co–N–C 164.3°), qualitatively consistent with an angle of 168.6° for the experimentally studied complex. Overall, the results suggest that, whereas alkylimido linkages are essentially linear, arylimido ones tend to be mildly bent.

Figures 4 and 5 present ground-state frontier MO energy level diagrams for the C_{3v} complexes **1** and **3**, respectively. An analogous diagram for **2** turned out too crowded (because of the lack of symmetry) and is therefore not shown. The diagrams clearly show that the ground states of these complexes may be described as $d_{\delta}^2 d_{\delta}^{\prime 2} d_{z^2}$. Given that the Co d_{z^2} -based MO is formally antibonding with respect to the Co–N_{imido} bond, the cobalt–imido linkage is best described as a double bond. However, *it is a very special double bond: it consists of two Co–N π -bonds but no formal σ -bond!*

As shown in Figures 4 and 5, the Co d_{z^2} -based MO has an unusual topology consisting of a swollen bottom lobe and a very shrunken top lobe; for the standard isodensity values used in Figures 4 and 5, the top lobe is actually engulfed by the middle lobe and is not directly visible. More precisely,

- (8) Ghosh, A.; Taylor, P. R. *Curr. Opin. Chem. Biol.* **2003**, *91*, 113–124.
- (9) Harvey, J. N. *Struct. Bonding* **2004**, *112*, 151–183.
- (10) The OPTX exchange functional: Handy, N. C.; Cohen, A. J. *Mol. Phys.* **2001**, *99*, 403–412.
- (11) The LYP correlation functional: Lee, C.; Yang, W.; Parr, R. G. *Phys. Rev. B* **1988**, *37*, 785–789.
- (12) Perdew, J. P.; Chevary, J. A.; Vosko, S. H.; Jackson, K. A.; Perderson, M. R.; Singh, D. J.; Fiolhais, C. *Phys. Rev. B* **1992**, *46*, 6671–6687.
- (13) The ADF program system was obtained from Scientific, Computing, and Modeling, Amsterdam, (<http://www.scm.com/>). For a description of the methods used in ADF, see: Velde, G. T.; Bickelhaupt, F. M.; Baerends, E. J.; Guerra, C. F.; Van Gisbergen, S. J. A.; Snijders, J. G.; Ziegler, T. J. *Comput. Chem.* **2001**, *22*, 2001.
- (14) Becke, A. D. *Phys. Rev. A* **1988**, *38*, 3098–3100.
- (15) Lee, C.; Yang, W.; Parr, R. G. *Phys. Rev. B* **1988**, *37*, 785–789.
- (16) Hammer, B.; Hansen, L. B.; Norskov, J. K. *Phys. Rev. B* **1999**, *59*, 7413–7421.
- (17) Zhang, Y.; Yang, W. *Phys. Rev. Lett.* **1998**, *80*, 890.

- (18) Adamo, C.; Barone, V. *J. Chem. Phys.* **2002**, *116*, 5933–5940.
- (19) Perdew, J. P.; Burke, K.; Ernzerhof, M. *Phys. Rev. Lett.* **1996**, *77*, 3865–3868.
- (20) Perdew, J. P.; Burke, K.; Ernzerhof, M. *Phys. Rev. Lett.* **1997**, *78*, 1396–1396.
- (21) Stephens, P. J.; Devlin, F. J.; Chabalowski, C. F.; Frisch, M. J. *J. Phys. Chem.* **1994**, *98*, 11623–11627.
- (22) Watson, M. A.; Handy, N. C.; Cohen, A. J. *J. Chem. Phys.* **2003**, *119*, 6475–6481.
- (23) Hertwig, R. H.; Koch, W. *Chem. Phys. Lett.* **1997**, *268*, 345–351.
- (24) Cohen, A. J.; Handy, N. C. *Mol. Phys.* **2001**, *99*, 607–615.

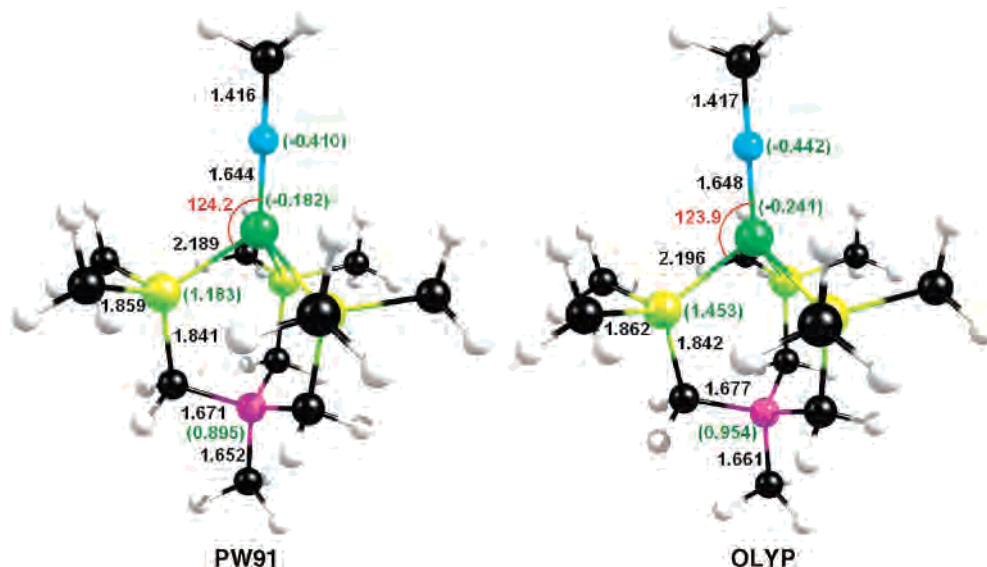


Figure 1. Selected PW91 and OLYP results for ground-state **1** (C_{3v}): optimized distances (Å, black), angles (deg, red), and Mulliken charges (green). Color code for atoms: C (black), N (cyan), H (ivory), Co (green), P (lime green), and B (magenta).

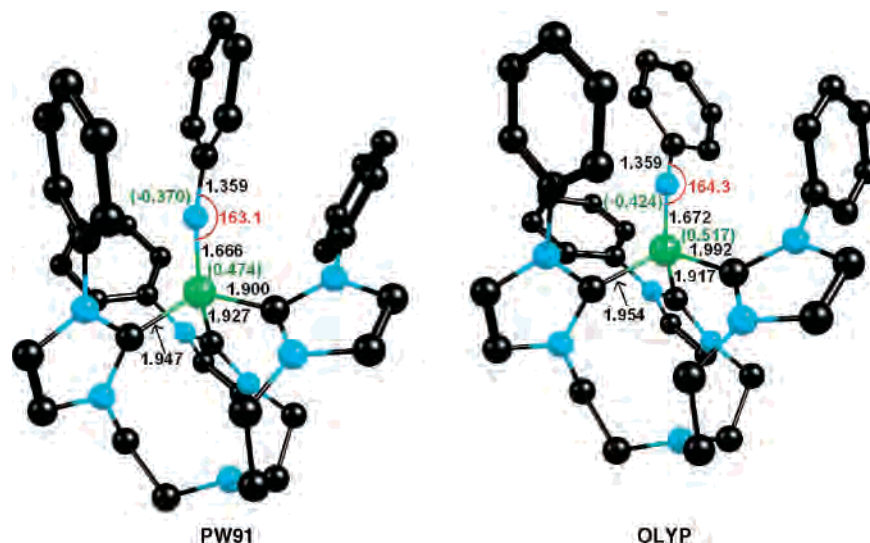


Figure 2. Selected PW91 and OLYP results for ground-state **2** (C_1): optimized distances (Å, black), angles (deg, red), and Mulliken charges (green). Color code for atoms: same as in Figure 1. Hydrogen atoms have been omitted for clarity.

this shape may be described as Co p_z and/or s character mixing in with the Co d_z^2 orbital. This s/p admixture may play a major role in minimizing the antibonding interaction of the Co d_z^2 orbital with the imido nitrogen.

Observe from Figures 4 and 5 that the ground-state HOMO–LUMO gaps of **1** (PW91 2.22 eV, OLYP 2.11 eV), **2** (PW91 1.49 eV, OLYP 1.35 eV), and **3** (PW91 1.23 eV, OLYP 1.03 eV) span a remarkably wide range of about 1 eV. These results (which may be viewed as qualitatively consistent with the spectrochemical series) provide some of the first insights into just how dramatically the supporting tripodal ligand can tune the HOMO–LUMO gaps and hence the spin-state energetics of Co^{III} –imido complexes. The HOMO–LUMO gaps provide a qualitative explanation of why the experimental analogue of **3** has a low-energy $S = 1$ state and hence exhibits spin-crossover behavior, as well as of why such behavior would be out of the question for **1**.⁴

A somewhat subtle point concerns the electronic configuration of the lowest-energy $S = 1$ state of **3**. Careful examination of the MO occupancies reveals that the lowest-energy triplet derives from a $d_\delta \rightarrow d_\pi$ excitation, rather than from a $d_z^2 \rightarrow d_\pi$ excitation. The mild bending of the imido linkage ($\angle \text{CoN}_{\text{imido}}\text{C}_{\text{imido}} = \sim 164^\circ$) in the $S = 1$ state (Figure 3) is then reasonably attributed to a Jahn–Teller distortion. Assuming approximate C_s symmetry, the electronic configuration of the lowest-energy $S = 1$ state of **3** may be described as follows.

d orbital symmetry occupancy	δ		σ	π	
	$d_{x^2-y^2}$ a'	d_{xy} a''	d_z^2 a'	d_{xz} a'	d_{yz} a''
	1	2	2	1	0

However, alternative $S = 1$ states are also likely to be low in energy.

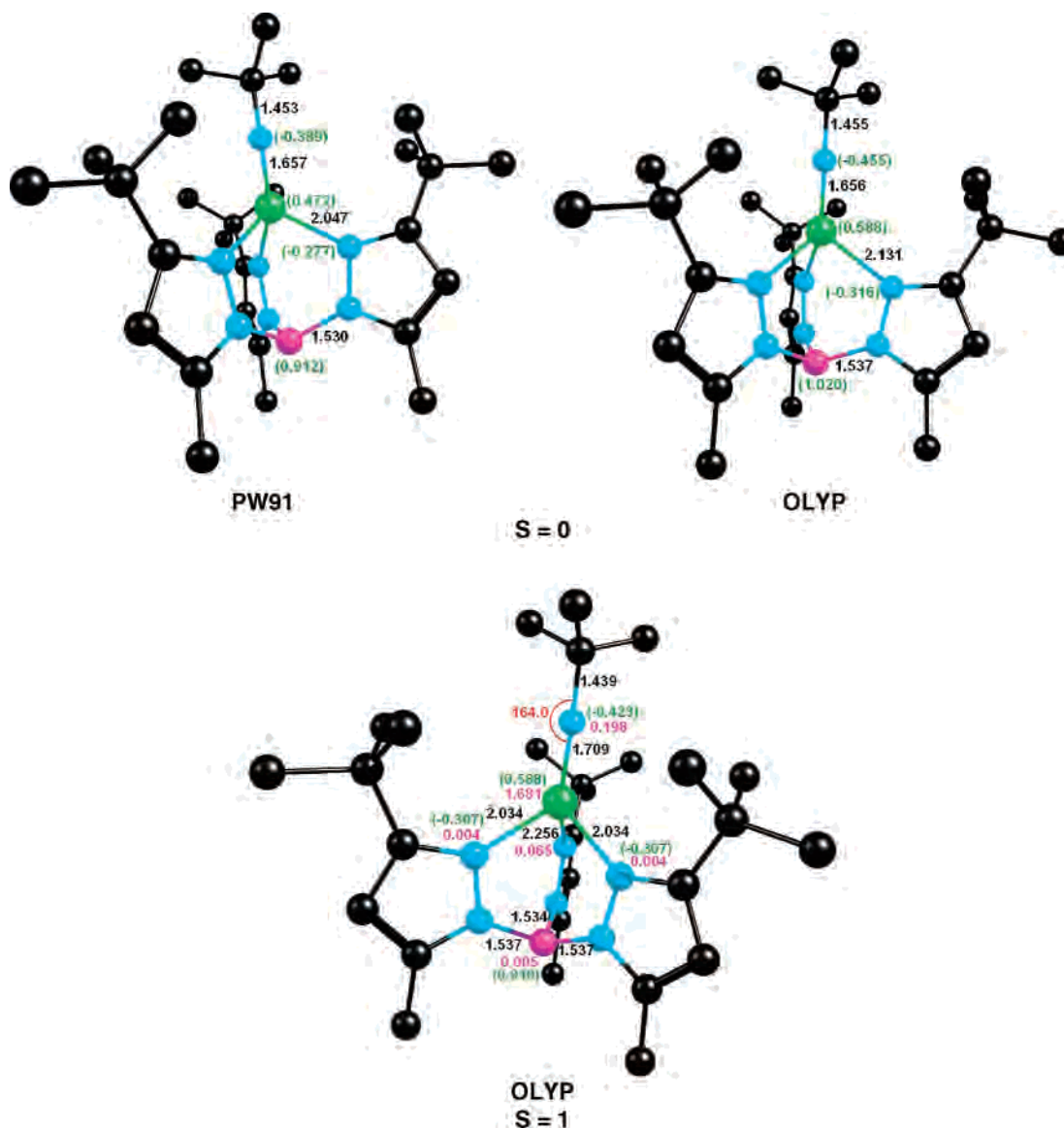


Figure 3. Selected PW91 and OLYP results for different spin states of **3**, $S = 0$ (C_{3v}) and 1 (C_1); optimized distances (Å, black) and angles (deg, red), Mulliken charges (green) and spin populations (magenta). Color code for atoms: same as in Figure 1. Hydrogen atoms (including the one on the boron) have been omitted for clarity.

b. Co(III)–Imido Spin-State Energetics. Table 1 presents the relative energies of the lowest-energy $S = 0$, 1 , and 2 states for **1**, **2**, and **3** for a number of pure and hybrid functionals. For **1** and **2**, all the functionals readily reproduce the observed $S = 0$ ground state, although the excited-state energetics are somewhat different. As elsewhere, the pure functionals examined seem to favor lower- S states, whereas the hybrid functionals B3LYP and O3LYP behave oppositely.^{8,9,25} The results on **3** afford a particularly discriminating view of the relative performance of the different functionals. Interestingly, whereas all the pure functionals examined correctly predict equienergetic $S = 0$ and 1 states for **3**, consistent with the spin-crossover behavior of Co^{III}–(Tp^t_{Bu,Me})₂(NAD),⁴ the B3LYP and O3LYP functionals predict $S = 2$ ground states that are over 0.5 eV below the $S = 0$ states. The tendency of hybrid functionals to unduly favor higher- S states has sometimes been corrected by adjusting

(typically lowering) the amount of exact exchange to around 15%, compared to the standard 20%.^{9,25a}

Unfortunately, the data in Table 1 do not allow us to narrow down our search for the best functional from the point

- (25) Selected studies comparing the performance of different functionals vis-à-vis transition metal spin-state energetics: (a) Reiher, M.; Salomon, O.; Hess, B. A. *Theor. Chem. Acc.* **2001**, *107*, 48–51. (b) Swart, M.; Groenhof, A. R.; Ehlers, A. W.; Lammertsma, K. *J. Phys. Chem. A* **2004**, *108*, 5479–5483. (c) Swart, M.; Ehlers, A. W.; Lammertsma, K. *Mol. Phys.* **2004**, *102*, 2467–2474. (d) Deeth, R. J.; Fey, N. *J. Comp. Chem.* **2004**, *25*, 1840–1848. (e) Groenhof, A. R.; Swart, M.; Ehlers, A. W.; Lammertsma, K. *J. Phys. Chem. A* **2005**, *109*, 3411–3417. (f) Daku, L. M. L.; Vargas, A.; Hauser, A.; Fouqueau, A.; Casida, M. E. *ChemPhysChem* **2005**, *6*, 1393–1410. (g) Ganzenmuller, G.; Berkaine, N.; Fouqueau, A.; Casida, M. E.; Reiher, M. *J. Chem. Phys.* **2005**, *122*, Art. No. 234321. (h) De Angelis, F.; Jin, N.; Car, R.; Groves, J. T. *Inorg. Chem.* **2006**, *45*, 4268–4276. (i) Vargas, A.; Zerara, M.; Krausz, E.; Hauser, A.; Daku, L. M. L. *J. Chem. Theory Comput.* **2006**, *2*, 1342–1359. (j) Rong, C. Y.; Lian, S. X.; Yin, D. L.; Shen, B.; Zhong, A. G.; Bartolotti, L.; Liu, S. B. *J. Chem. Phys.* **2006**, *125*, Art. No. 174102. (k) Strickland, N.; Harvey, J. N. *J. Phys. Chem. B* **2007**, *111*, 841–852.

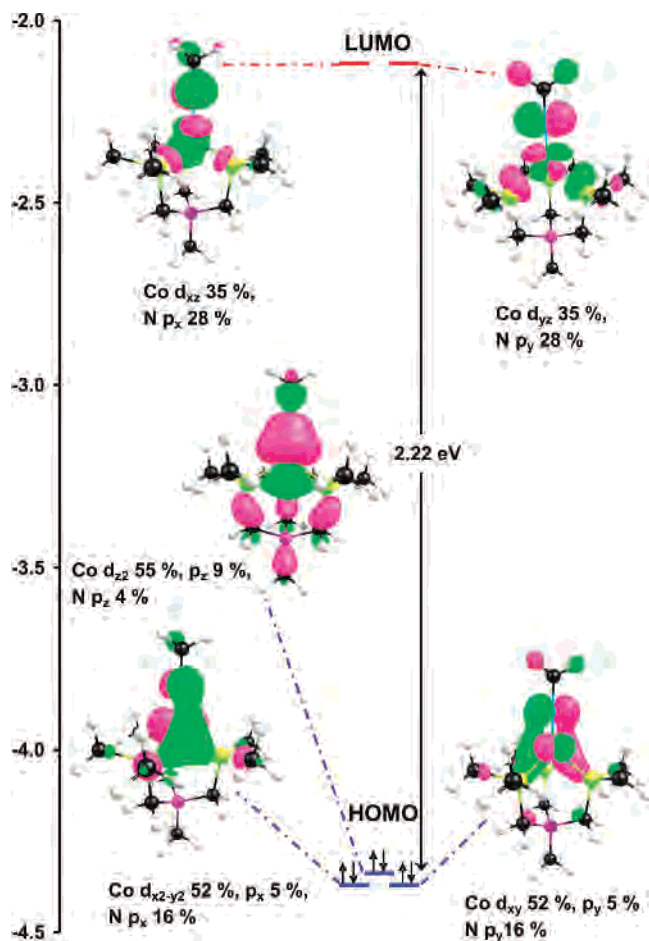


Figure 4. PW91 MO energy level (eV) diagram for ground-state ($S = 0$) 1.

of view of transition metal spin-state energetics. To do so, we can draw on a recent multifunctional study of first-row transition metal–nacnac–imido complexes.³ It turned out that only the newer pure functionals OLYP and OPBE, based on Handy and Cohen’s OPTX exchange functional, correctly reproduced the experimentally observed spin states for *both* Fe^{III} ($S = 3/2$)²⁶ and Co^{III} ($S = 0$)⁷ nacnac–imido complexes.³ In contrast, older pure functionals such as PW91 predicted $S = 1/2$ ground states or at best equienergetic $S = 1/2$ and $3/2$ states for Fe^{III}–nacnac–imido derivatives, whereas hybrid functionals, as in this study, predicted $S = 1$ or 2 ground states for the Co^{III}–imido complexes.³ We would therefore like to propose that the OLYP and OPBE data in Table 1 are our “best” predictions for the spin-state energetics of the pseudotetrahedral Co^{III}–imido complexes studied. We have also checked that the data in Table 1 are essentially converged to the basis set limit; expansion of the basis set to TZ2P results in minimal changes to the energetics.

c. Exploratory Studies on Other Pseudotetrahedral First-Row Imido Complexes. Encouraged by the performance of the OLYP and OPBE functionals,³ we have carried out an exploratory study of pseudotetrahedral Cr(III), Mn(III), and Fe(III) imido (N^tBu) complexes with the mebp3

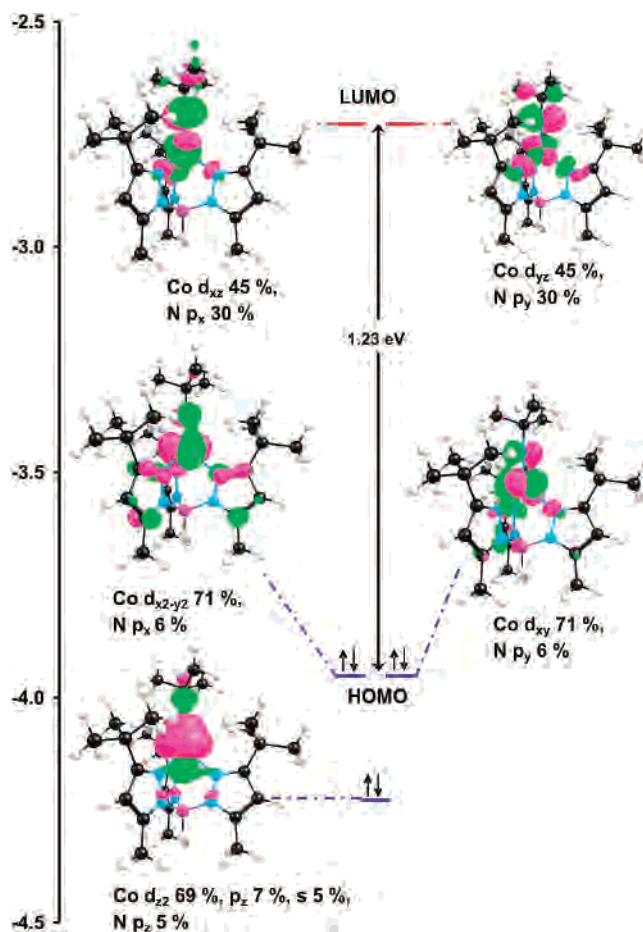


Figure 5. PW91 MO energy level (eV) diagram for ground-state ($S = 0$) 3.

and Tp^tBu,Me supporting ligands, the goal being not only to study the role of the supporting ligand in modulating the spin-state energetics but also to identify novel targets for chemical synthesis. Table 2 presents calculated spin-state energetics data for these complexes. In addition, Figure 6 presents highlights of optimized geometries (distances and angles), Mulliken charges and spin populations for the lower-energy spin states of the various Tp complexes. Some of the more notable results may be summarized as follows.

1. Cr^{III}(mebp3)(NMe) and Cr^{III}(Tp^tBu,Me)(N^tBu). Perhaps not surprisingly, a perfectly threefold-symmetric, $S = 3/2$ ground state is clearly indicated for both complexes. The $d_3^1 d_0^1 d_z^1$ configuration suggests that most of the excess spin density should be localized on the Cr, which is indeed the case, albeit with a twist. As shown in Figure 6, a cylindrically symmetric disc of minority spin density resides on the imido nitrogen. Careful examination of the valence MOs indicates that the excess minority spin results from a slight spatial offset between the α - and β -spin forms of the d_{π} – p_{π} bonding MOs. Such spatially offset π -bonding is actually relatively common in open-shell transition-metal complexes, and we have seen a similar occurrence in an NO complex, Mo(P)(NO)(MeOH) (P = porphyrin), which has an {MoNO}⁵ $d_{\pi}^2 d_{\sigma}^2 d_z^1$ configuration but, nonetheless, exhibits a significant amount of minority spin density on the NO.²⁷

(26) Eckart, N. A.; Vaddadi, S.; Stoian, S.; Lachicotte, R. J.; Cundari, T. R.; Holland, P. L. *Angew. Chem., Int. Ed.* **2006**, *45*, 6868–6871.

Table 1. Calculated Relative Energies (eV) of the Lowest-Energy $S = 0, 1,$ and 2 States of **1, 2,** and **3**

complex	S	optimizations		single-point energies for PW91 geometries							
		PW91	OLYP	BLYP	RPBE	revPBE	mPBE	OPBE	B3LYP	O3LYP	
1	0	0.00	0.00	0.00	0.00	0.00	0.00	0.00	0.00	0.00	0.00
1	1	0.94	0.75	0.83	0.83	0.85	0.91	0.90	0.64	0.72	
1	2	1.71	1.27	1.48	1.45	1.51	1.64	1.52	0.80	0.98	
2	0	0.00	0.00	0.00	0.00	0.00	0.00	0.00	0.00	0.00	
2	1	0.51	0.32	0.43	0.40	0.42	0.47	0.43	0.14	0.21	
2	2	0.97	0.41	0.77	0.68	0.73	0.88	0.64	−0.10	0.05	
3	0	0.00	0.00	0.00	0.00	0.00	0.00	0.00	0.00	0.00	
3	1	0.21	−0.05	0.16	0.06	0.09	0.16	0.00	−0.24	−0.20	
3	2	0.24	0.20	0.17	−0.03	0.02	0.15	−0.24	−0.65	−0.68	

Table 2. Calculated Relative Energies (eV) of Selected Lowest-Energy Spin States of $M^{III}(Tp^{tBu,Me})(N^tBu)$ and $M^{III}(mebp3)(NMe)$ Complexes Where $M = Cr, Mn,$ and Fe^d

metal	supp. ligand	point group	S	optimizations		single-point energies for OLYP geometries						
				OLYP	PW91	BLYP	RPBE	revPBE	mPBE	OPBE	B3LYP	O3LYP
Cr	$Tp^{R,R'}$	C_s	1/2	1.17	0.83	0.78	0.93	0.91	0.86	1.29	1.08	1.37
Cr	$Tp^{R,R'}$	C_{3v}	3/2	0.00	0.00	0.00	0.00	0.00	0.00	0.00	0.00	0.00
Mn	$Tp^{R,R'}$	C_{3v}	0	2.40	1.51	1.48	1.92	1.85	1.65	2.58	4.12	3.96
Mn	$Tp^{R,R'}$	C_s	1	0.76	0.26	0.23	0.47	0.44	0.34	0.86	0.96	1.17
Mn	$Tp^{R,R'}$	C_s	2	0.00	0.00	0.00	0.00	0.00	0.00	0.00	0.00	0.00
Fe	$Tp^{R,R'}$	C_s	1/2	0.75	0.05	0.01	0.31	0.27	0.15	0.85	0.81	1.16
Fe	$Tp^{R,R'}$	C_s	3/2	0.32	0.04	0.01	0.12	0.11	0.07	0.37	0.25	0.44
Fe	$Tp^{R,R'}$	C_{3v}	5/2	0.00	0.00	0.00	0.00	0.00	0.00	0.00	0.00	0.00
Cr	mebp3	C_s	1/2	0.98	0.72	0.68	0.82	0.80	0.74	1.06	0.96	1.15
Cr	mebp3	C_{3v}	3/2	0.00	0.00	0.00	0.00	0.00	0.00	0.00	0.00	0.00
Mn	mebp3	C_{3v}	0	0.38	0.32	0.34	0.40	0.38	0.35	0.38	0.77	0.60
Mn	mebp3	C_s	1	0.00	0.00	0.00	0.00	0.00	0.00	0.00	0.00	0.00
Mn	mebp3	C_s	2	0.41	0.96	0.78	0.67	0.72	0.86	0.47	−0.01	−0.03
Fe	mebp3	C_s	1/2	0.00	0.00	0.00	0.00	0.00	0.00	0.00	0.00	0.00
Fe	mebp3	C_s	3/2	0.70	1.04	0.86	0.82	0.86	0.96	0.84	0.22	0.37
Fe	mebp3	C_{3v}	5/2	1.03	1.79	1.48	1.37	1.45	1.65	1.25	0.33	0.46

^d The point groups indicated were carefully determined, based on comparison of optimized geometries with C_{3v} , C_s , and C_1 symmetry constraints.

2. $Mn^{III}(mebp3)(NMe)$ and $Mn^{III}(Tp^{tBu,Me})(N^tBu)$. Lu and Peters have recently reported a number of pseudotetrahedral Mn–trisphosphinoborate complexes, although their initial efforts to generate trisphosphine-based Mn–imido and –nitrido species have not been successful so far.²⁸ However, the authors conjecture that the synthetic challenges involved should be surmountable. In the same vein, Mn–Tp–imido complexes are as yet unknown. Assuming that the OLYP (or OPBE) GGA yields the most reliable spin-state energetics, our results (Table 2) indicate that, whereas $Mn^{III}(mebp3)(NMe)$ should exhibit an $S = 1$ ground state, its $Tp^{tBu,Me}$ analogue should be $S = 2$. As shown in Figure 6, the unoccupied d_{xy} orbital in the d^4 $Mn^{III}(Tp^{tBu,Me})(N^tBu)$ complex results in a highly anisotropic spin density profile around the Mn–N_{imido} linkage, very similar to what we found earlier for an $Mn^{III}(nacnac)(NMe)$ complex.³

3. $Fe^{III}(mebp3)(NMe)$ and $Fe^{III}(Tp^{tBu,Me})(N^tBu)$. A number of well-characterized phosphinoborate-supported Fe–imido/nitrido species have been reported in recent years by Peters and co-workers;¹ in addition, these complexes have been the subject of a recent, comprehensive DFT study.² In

contrast, Fe–Tp–imido complexes are as yet unknown. As noted before,² the $Fe^{III}(mebp3)(NMe)$ model complex is an $S = 1/2$ species, with a mild bending of the imido linkage. Table 2 indicates that the higher-spin states are several tenths of an electronvolt higher in energy relative to the low-spin ground state. Use of the $Tp^{tBu,Me}$ supporting ligand instead of mebp3 results in a complete reversal of the spin-state energetics. Our best estimates (OLYP and OPBE) suggest an $S = 5/2$ ground state for $Fe^{III}(Tp^{tBu,Me})(N^tBu)$, separated from $S = 3/2$ and $1/2$ states by clear margins of energy. In addition, as shown in Figure 6, our calculations predict a perfectly C_{3v} -symmetric structure and a cylindrically symmetric spin density profile for the $S = 5/2$ ground state. Given that theoretical studies are often relegated to rationalizing experimental observations after the fact, it will be an exciting vindication of our approach if certain of the above predictions are borne out by experiment.

Conclusion

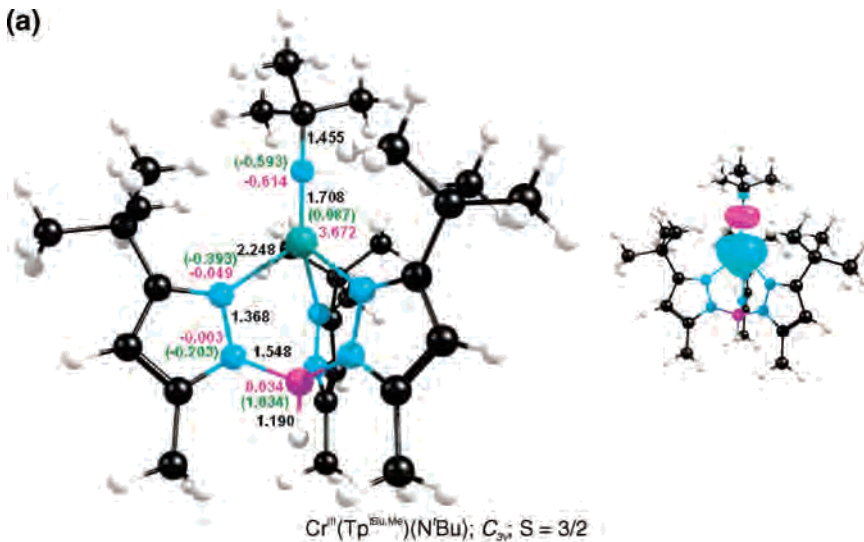
Our main findings may be enumerated as follows.

1. The tripodal supporting ligand plays a crucial role in tuning the spin-state energetics of pseudotetrahedral

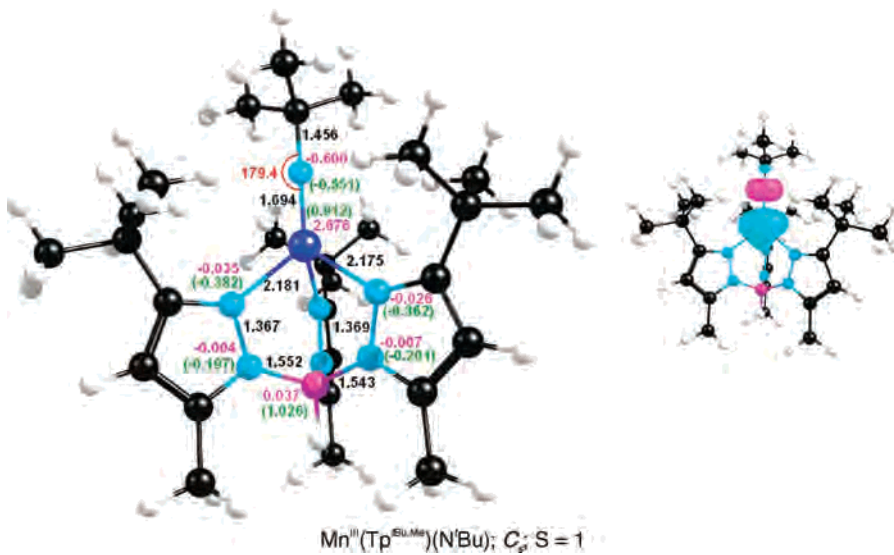
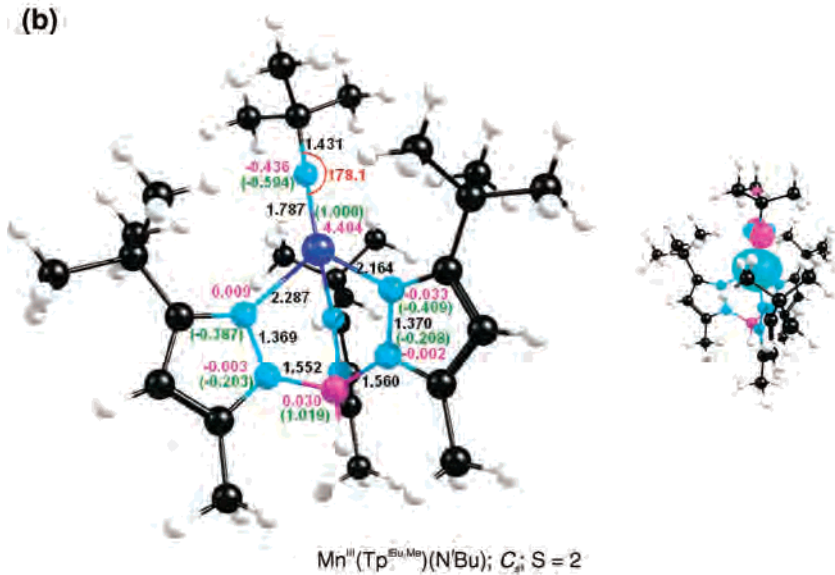
(27) Tangen, E.; Ghosh, A. *J. Inorg. Biochem.* **2005**, *99*, 959–962.

(28) Lu, C. C.; Peters, J. C. *Inorg. Chem.* **2006**, *45*, 8597–8607.

(a)



(b)



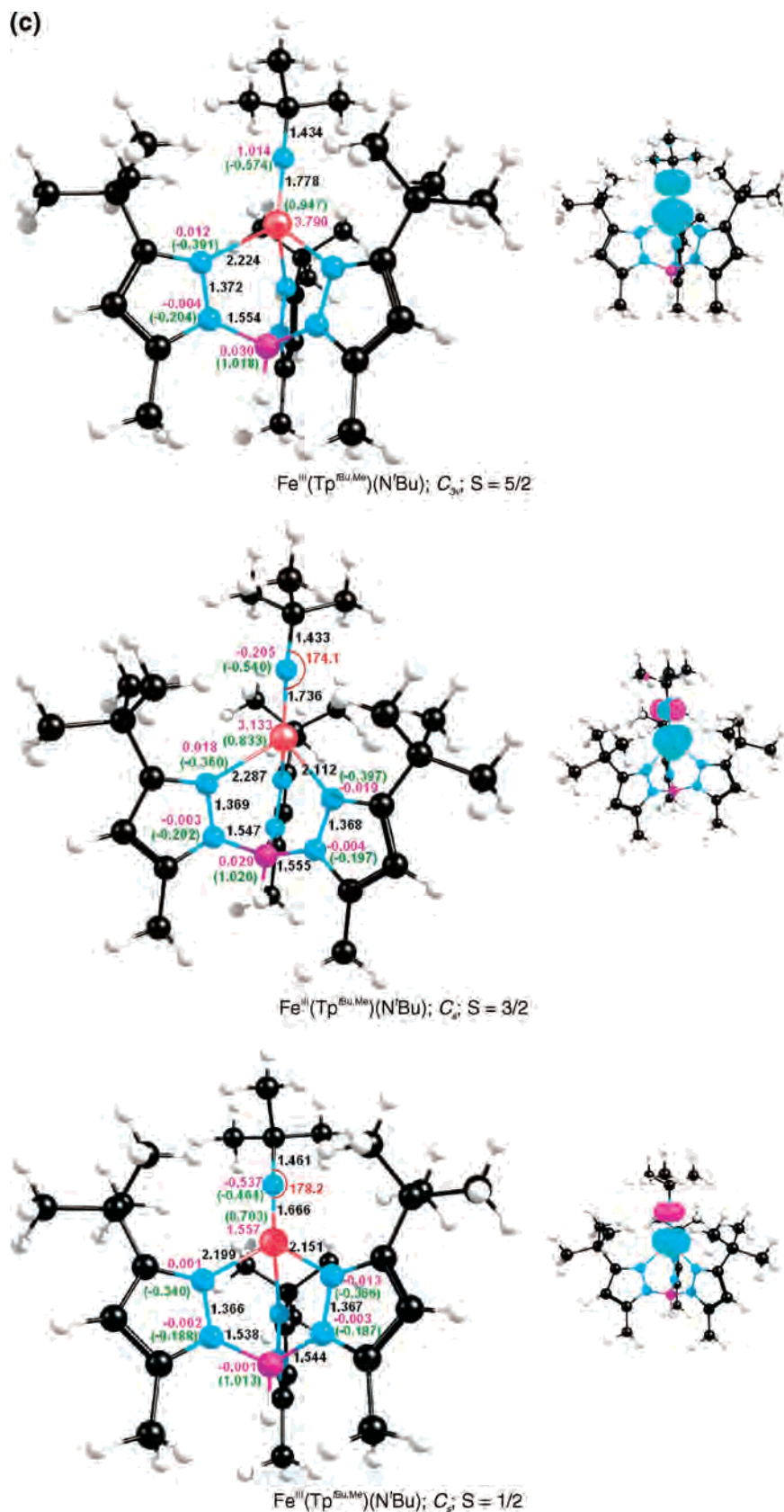


Figure 6. Highlights of OLYP results for M^{III}(Tp^{Bu,Me})(N'Bu) complexes: (a) M = Cr, (b) M = Mn, and (c) M = Fe. Optimized distances (Å, black), angles (deg, red), Mulliken charges (green), and spin populations (magenta) are presented to the left of each row, while a spin density plot (majority spin, cyan; minority spin, magenta) is included on the right-hand side. Color code for atoms: same as in Figure 1.

Co^{III}–imido complexes. The HOMO–LUMO gaps vary enormously between **1** and **3** and are in the order trisphos-

phine (**1**) \gg triscarbene (**2**) > hydrotris(pyrazolyl)borate (**3**). Thus, whereas **3** is predicted to exhibit spin-crossover

behavior, the lowest-energy $S = 1$ state of **1** is about 0.75 eV above the ground state (OLYP).

2. On the DFT methodological front, this present study has afforded valuable calibration data on the performance of different functionals vis-à-vis the spin-state energetics of transition metal complexes. In a recent study,⁴ we found evidence that the newer OPTX-based¹⁰ functionals OLYP and OPBE may be among the best functionals in this regard.³ If that is indeed the case, then our OLYP (and OPBE) results provide the best estimates so far of the spin-state energetics of the Co^{III}–imido complexes studied.

3. Exploratory studies of additional first-row imido complexes have led to a number of interesting predictions. Thus, whereas an $S = 1$ ground state is predicted for

trisphosphine–Mn^{III}(NR) complexes, Mn^{III}(Tp)(NR) derivatives are predicted to be $S = 2$. In the same vein, whereas trisphosphine–Fe^{III}(NR) complexes are known to be $S = 1/2$,¹ Fe^{III}(Tp)(NR) derivatives are predicted to exhibit $S = 5/2$ ground states, separated from lower-spin states by a clear margin of energy.

Acknowledgment. This work was supported by the Research Council of Norway. We thank Prof. Klaus Theopold for sharing ref 4b with us prior to publication.

Supporting Information Available: Optimized coordinates of key species studied (45 pages). This material is available free of charge via the Internet at <http://pubs.acs.org>.

IC700543F